Inhibition of Integrin αvβ6, an Activator of Latent Transforming Growth Factor-β, Prevents Radiation-induced Lung Fibrosis

Khalid Puthawala[1]*, Nicos Hadjiangelis[1]*, Steven C. Jacoby[1]*, Emmanuel Bayongan[1]*, Zhicheng Zhao[2], Zhiwei Yang[2], Mary Louise Devitt[3], Gerald S. Horan[4], Paul H. Weinreb[4], Matvey E. Lukashev[4], Shelia M. Violette[4], Kristen S. Grant[2], Cristina Colarossi[2], Silvia C. Formenti[3], and John S. Munger[1,2]

Departments of [1]Medicine, [2]Cell Biology, and [3]Radiation Oncology, New York University School of Medicine, New York, New York; and [4]Biogen Idec, Cambridge, Massachusetts

***Rationale*: In experimental models, lung fibrosis is dependent on transforming growth factor (TGF)-β signaling. TGF-β is secreted in a latent complex with its propeptide, and TGF-β activators release TGF-β from this complex. Because the integrin αvβ6 is a major TGF-β activator in the lung, inhibition of αvβ6-mediated TGF-β activation is a logical strategy to treat lung fibrosis.**

***Objectives*: To determine, by genetic and pharmacologic approaches, whether murine radiation-induced lung fibrosis is dependent on αvβ6.**

***Methods*: Wild-type mice, αvβ6-deficient (*Itgb6*$^{-/-}$) mice, and mice heterozygous for a *Tgfb1* mutation that eliminates integrin-mediated activation (*Tgfb1*$^{+/RGE}$) were exposed to 14 Gy thoracic radiation. Some mice were treated with an anti-αvβ6 monoclonal antibody or a soluble TGF-β receptor fusion protein. αvβ6 expression was determined by immunohistochemistry. Fibrosis, inflammation, and gene expression patterns were assessed 20–32 weeks postirradiation.**

***Measurements and Main Results*: β6 Integrin expression increased within the alveolar epithelium 18 weeks postirradiation, just before onset of fibrosis. *Itgb6*$^{-/-}$ mice were completely protected from fibrosis, but not from late radiation-induced mortality. Anti-αvβ6 therapy (1–10 mg/kg/wk) prevented fibrosis, but only higher doses (6–10 mg/kg/wk) caused lung inflammation similar to that in *Itgb6*$^{-/-}$ mice. *Tgfb1*-haploinsufficient mice were also protected from fibrosis.**

***Conclusions*: αvβ6-Mediated TGF-β activation is required for radiation-induced lung fibrosis. Together with previous data, our results demonstrate a robust requirement for αvβ6 in distinct fibrosis models. Inhibition of αvβ6-mediated TGF-β activation is a promising new approach for antifibrosis therapy.**

Keywords: inflammation; lymphocyte; monoclonal antibody

AT A GLANCE COMMENTARY

Scientific Knowledge on the Subject

Transforming growth factor (TGF)-β is a profibrotic cytokine, and its latent form is activated by the integrin αvβ6 in the lung. A monoclonal antibody has been developed that potently and specifically inhibits αvβ6.

What This Study Adds to the Field

Inhibition of αvβ6-mediated TGF-β activation prevents murine radiation–induced lung fibrosis, and the antifibrotic effect is achieved at doses lower than those that cause lung inflammation due to loss of TGF-β's immunomodulatory effects.

Lung fibrosis occurs when injury is followed by disordered matrix remodeling (1). The cytokine, transforming growth factor (TGF)-β, affects multiple processes involved in this response (e.g., matrix production, epithelial cell apoptosis, epithelial–mesenchymal transition, fibroblast phenotype, and protease activity), and its activity is required for several types of experimental fibrosis (2, 3). Inhibition of TGF-β signaling is therefore being intensely investigated as an antifibrosis therapy.

Of three TGF-β isoforms, TGF-β1 likely has the most important role in fibrosis. TGF-β genes encode a C-terminal TGF-β sequence and an N-terminal prodomain called latency-associated peptide (LAP). TGF-β and LAP are secreted as a complex in which TGF-β is latent (i.e., unable to bind to TGF-β receptors). LAP also interacts with proteins of the latent TGF-β binding protein family, which anchor latent TGF-β to the extracellular matrix (4). Release of TGF-β from LAP (TGF-β activation) is a highly regulated step in TGF-β signaling (5).

Putative TGF-β activators include proteases that degrade LAP (6, 7), thrombospondin-1 (8, 9), reactive oxygen species (10), and the integrins αvβ6 and αvβ8, which interact with the amino acid sequence arginine–glycine–aspartic acid (RGD) located near the C terminus of TGF-β1–LAP and TGF-β3–LAP (11–13). Integrin-mediated TGF-β1 activation is required for TGF-β1's roles in vasculogenesis, immune tolerance, and formation of Langerhans cells (14).

In the lung, αvβ6 is expressed at a low level in normal epithelium and is up-regulated after injury. Mice lacking αvβ6 because of a deletion mutation in the β6 subunit gene (*Itgb6*$^{-/-}$) are healthy in most respects, but have lung inflammation similar to that in TGF-β1–null mice and delayed-onset emphysema due to loss of TGF-β–mediated suppression of matrix metalloproteinase-12 expression by alveolar macrophages (AMs) (15, 16). Intratracheal administration of bleomycin causes an acute lung injury and a rapid fibrotic response; both the early capillary leak and the fibrosis in this model are dependent upon TGF-β signaling and expression of αvβ6 (13, 17). These observations raise the possibility that αvβ6 inhibition might prevent lung fibrosis without eliminating all TGF-β signaling, as shown in a kidney model (18).

(*Received in original form June 1, 2007; accepted in final form October 4, 2007*)

Supported by National Institutes of Health grants HL077526 and HL063786 and by a research grant from Biogen Idec (J.S.M.).

*These investigators contributed equally to this article.

Correspondence and requests for reprints should be addressed to John S. Munger, M.D., New York University School of Medicine, Department of Cell Biology, MSB607, 550 First Avenue, New York, NY 10282. E-mail: john.munger@med.nyu.edu

This article has an online supplement, which is accessible from this issue's table of contents at www.atsjournals.org

Am J Respir Crit Care Med Vol 177. pp 82–90, 2008
Originally Published in Press as DOI: 10.1164/rccm.200706-806OC on October 4, 2007
Internet address: www.atsjournals.org

We examined the role of αvβ6 in the radiation-induced lung fibrosis (RILF) model. In contrast to bleomycin-induced fibrosis, RILF is delayed in onset, occurring 20 weeks or longer after radiation injury, and is not contemporaneous with acute injury or severe inflammation. We chose this model to test whether αvβ6 is involved in mechanistically distinct lung fibrosis models, and in order to test the effect of therapy given during the fibrotic response but not during the initial lung injury. Our results indicate that αvβ6 plays a robust role in distinct forms of lung fibrosis and is a promising target for therapeutics.

METHODS

Lung Irradiation

Mice were C57BL/6J females. Mice with a mutation in *Tgfb1* exon 5 that encodes arginine–glycine–glutamic acid (RGE) instead of arginine–glycine–aspartic acid at the integrin-binding site of TGF-β1–LAP were generated as previously described (14) and backcrossed 10 generations onto the C57BL/6J background; $Tgfb1^{+/+}$ and $Tgfb1^{+/RGE}$ littermates were used for irradiation. $Itgb6^{-/-}$ mice backcrossed to the C57BL/6J background were from Dean Sheppard (University of California, San Francisco). Mice (8–10 wk old) were anesthetized with Avertin and exposed to 14 Gy radiation to the thorax from a ^{60}Co source. The New York University School of Medicine animal care committee approved all procedures, which conformed to National Institutes of Health (Bethesda, MD) guidelines.

Lung, Blood, and Bronchoalveolar Lavage Fluid Procedures

Lungs from dead or moribund mice were inflated with 800 μl 10% formalin. In anti-αvβ6 monoclonal antibody (mAb) experiments, lungs were lavaged twice with 700 μl phosphate-buffered saline (PBS). The right mainstem bronchus was ligated and the right lungs frozen in liquid N_2. The left lung was inflated with 400 μl 10% formalin. Left lungs were cut transversely into 5-μm sections and stained with Masson's trichrome. Aliquots of bronchoalveolar lavage (BAL) fluid were used for cell counts and cytospins, and the remainder frozen in liquid N_2. Immunohistochemical detection of β6 protein with the anti-β6 chimeric mAb, 2A1, was as previously described (18). The percent fibrosis area (%FA) was calculated as previously described (19) using ImageJ software (National Institutes of Health). For $Tgfb1^{+/+}$ and $Tgfb1^{+/RGE}$ mice, %FA was measured using both left and right lung from each mouse. The measurement of hydroxyproline content was as previously described (20).

Antibody Treatments

The inhibitory anti-αvβ6 mAb, 6.3G9, isotype control antibody, 1E6, and recombinant soluble TGF-β receptor II-Fc fusion protein (rsTGF-βRII-Fc) have previously been described (18, 21). Antibodies were injected weekly, either intraperitoneally (first experiment) or subcutaneously. Injection volumes were 200 μl.

Right:Left Ventricle Mass Ratio Measurement

Hearts from mice that died between 28 and 32 weeks postirradiation were compared with hearts from mice killed at 32 weeks postirradiation or from 7 unirradiated C57BL/6J mice. The right ventricular free wall (RV) was dissected from the left ventricle and septum (LV), and individual pieces were weighed.

Multiplex Analysis of BAL Fluid Proteins

BAL fluid aliquots were analyzed by Rules-Based Medicine, Inc. (Austin, TX), for a standard panel of 60 mouse proteins (http://www.rulesbasedmedicine.com/) using dyed microspheres permeated with capture antibodies specific for each target analyte (Luminex, Austin, TX).

RNA Isolation

Total RNA was prepared from lungs stored at −80°C using the Qiazol reagent (Qiagen, Valencia, CA) according to the manufacturer's protocol. The RNA quality was verified by capillary electrophoresis on Bioanalyzer 2100 (Agilent, Santa Clara, CA).

Design of Primers, Probes, and Oligonucleotide Standard Templates for Taqman

Oligonucleotide primers and Taqman minor groove binder (MGB) probes were designed from Affymetrix (Santa Clara, CA) consensus sequences using Primer Express version 2.0.0 (Applied Biosystems, Inc., Foster City, CA). Taqman MGB probes were designed with a 5′ fluorescent reporter dye, 6-carboxy-fluorescein (FAM), and a 3′ MGB/nonfluorescent quencher (MGBNF). Oligonucleotide standard templates were designed by the addition of 10 bp of gene-specific sequence to the 5′ and 3′ ends of the amplicon. Reverse-phase HPLC–urified primers and oligonucleotide standard templates were purchased from Biosearch Technologies Inc. (Novato, CA). HPLC-purified primers and probe for murine glyceraldehyde-3-phosphate dehydrogenase were synthesized at Biogen Idec (sequences CATGGCCTTCCGTGTTCCTA, GCGGCACGTCAGATCC, and 6FAM-CCCCAATGTGTCCGTC).

Taqman Thermal Cycling

Quadruplicate polymerase chain reactions for samples and standards were cycled in a 7900HT (Applied Biosystems, Inc.) thermal cycler under the following conditions: 50°C for 2 minutes, 95°C for 10 minutes, and 40 cycles of 95°C for 15 seconds and 60°C for 60 seconds. The fluorescence emission was collected every 7 seconds for each reaction well. Relative transcript quantities were determined for each sample by comparison to oligonucleotide standard curve using Sequence Detection Software (Applied Biosystems, Inc.)

Microarray Procedures

The quality of RNA samples (minimum 5 per experimental group) was verified by capillary electrophoresis on a Bioanalyzer 2000 (Agilent). Hybridization probes were prepared from individual RNA samples and profiled on separate Mouse Genome 430 2.0 oligonucleotide arrays (Affymetrix). Hybridization probe synthesis, hybridization, and microarray scanning were performed using the manufacturer's protocols. The array scans were converted into Affymetrix .CEL files and the resulting data set (group of .CEL files representing the complete experiment) was normalized using the GC content–adjusted robust microarray average method. Statistical and clustering analyses were done using the GeneSpring (Agilent) software. We used two-step *t* test filtering to identify probesets whose signal intensity was altered, first, when comparing irradiated, PBS-treated mice to the aged, unirradiated control group ($P < 0.001$) and, second, when comparing irradiated, PBS-treated mice and irradiated mice treated with 1 mg/kg 6.3G9 ($P < 0.05$; n = 3 for the PBS-treated radiation group, and n = 5–8 for the other groups tested). Functional annotation of selected gene lists was done using the Ingenuity Pathways Analysis database (Ingenuity, Redwood City, CA).

Statistical Analysis

Significance of the differences between mean %FA of different treatment groups was assessed by the Mann-Whitney U test. Differences between mean hydroxyproline concentrations or mean RV:LV ratios were evaluated with Student's *t* test. Mean values of measurements are displayed with error bars indicating SEM. Statistical comparisons of protein levels in the BAL fluid were made between vehicle control and/or isotype control, and various doses of test article using one-way analysis of variance. When statistically significant differences were established, significant differences between groups were evaluated by Dunnet's multiple comparison test (significance defined as $P < 0.05$).

RESULTS

Increased Expression of αvβ6 by Alveolar Epithelium Is a Late Event after Radiation Injury

The αvβ6 integrin is normally expressed at a low level in lung epithelium, but can be up-regulated by injury and inflammation. At 2-week intervals postirradiation, we assessed β6 integrin expression by immunohistochemical staining with an mAb that recognizes the β6 subunit. β6 expression did not change from baseline low levels until a sharp increase 18–20 weeks postirradiation throughout the alveolar epithelium (Figure 1A and

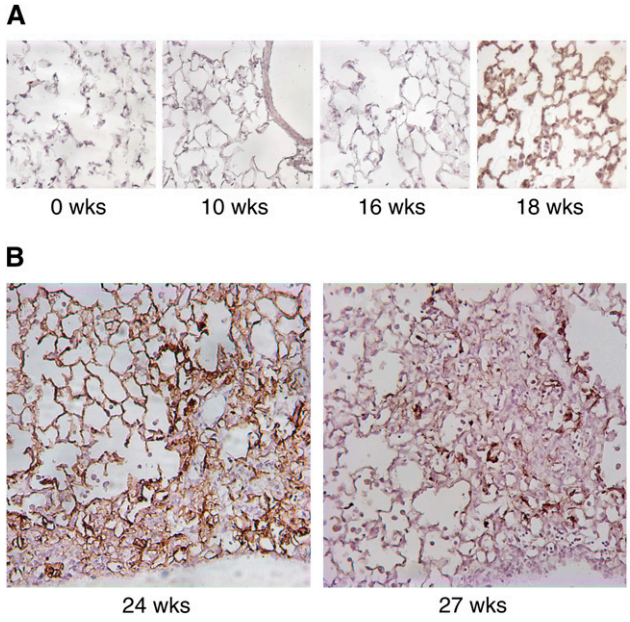

Figure 1. αvβ6 Expression in the lung after irradiation. (*A*) Lungs of irradiated wild-type mice were immunostained with an antibody (ch2A1) specific for the β6 integrin subunit. αvβ6 expression increases at 18 weeks postirradiation. (*B*) The αvβ6 is highly expressed in fibrotic areas. At 24 weeks postirradiation, immunostaining is also intense in nonfibrotic areas. At 27 weeks postirradiation, immunostaining is less evident in nonfibrotic areas, but remains intense in cells within fibrotic lesions.

data not shown). Areas of fibrosis first became apparent 20–22 weeks postirradiation (data not shown). At 24 weeks postirradiation, β6 expression was prominent throughout alveolar epithelium in nonfibrotic areas and in epithelial cells within regions of fibrosis, which were located subpleurally; by 27 weeks postirradiation and later, intensely positive β6 expression persisted in epithelial cells within fibrotic areas, but often became less prominent in nonfibrotic areas (Figure 1B and data not shown).

Mice Lacking αvβ6 Do Not Develop RILF

The close temporal and spatial association between αvβ6 expression and RILF lesions supports the idea that αvβ6-mediated TGF-β activation is involved in the fibrotic process. To determine whether αvβ6 is necessary for development of RILF, we compared the fibrotic responses of irradiated *Itgb6*$^{+/+}$ and *Itgb6*$^{-/-}$ mice. In *Itgb6*$^{+/+}$ lungs (Figure 2A), fibrotic areas were well demarcated and subpleural. We observed fibrotic areas in sections from 21 of 23 *Itgb6*$^{+/+}$ mice killed 24–28 weeks postirradiation (mean, 26.0 wk postirradiation), but found no fibrotic areas in any of 17 lung sections from *Itgb6*$^{-/-}$ mice 26–28 weeks postirradiation (mean, 27.1 wk postirradiation), a difference that is statistically significant ($P = 0.001$, Fisher's exact test). The %FA of sections from *Itgb6*$^{+/+}$ mice (27 wk after irradiation) was 17 ± 3%. Analysis of additional sections from *Itgb6*$^{-/-}$ mice did not reveal fibrotic areas, confirming the report by Haston and colleagues that analysis of a single lung section per mouse is adequate for assessment of fibrosis (19). We confirmed the histologic findings by measuring the hydroxyproline content of lungs from *Itgb6*$^{+/+}$ and *Itgb6*$^{-/-}$ mice 27 weeks postirradiation (Figure 2B).

After 14 Gy of thoracic irradiation, mortality was negligible until 18–20 weeks postirradiation and reached 50% at 26 weeks postirradiation (Figure 2C). There was no significant difference in survival of *Itgb6*$^{+/+}$ and *Itgb6*$^{-/-}$ mice. These survival curves are similar to previous results for female C57BL/6 mice (19).

An Inhibitory Anti-αvβ6 mAb and a TGF-β Antagonist Prevent RILF

The effect of blocking TGF-β signaling during the late radiation-induced fibrosis phase has not been defined. To address this issue, we initiated treatment 16 weeks postirradiation, just prior to the up-regulation of αvβ6, with the anti-αvβ6 mAb 6.3G9, a specific and potent inhibitor of αvβ6 able to prevent αvβ6-mediated TGF-β activation (21). In addition, we treated mice with rsTGF-βRII-Fc, which inhibits active TGF-β (18). Fibrosis was assessed in mice that died more than 20 weeks post-

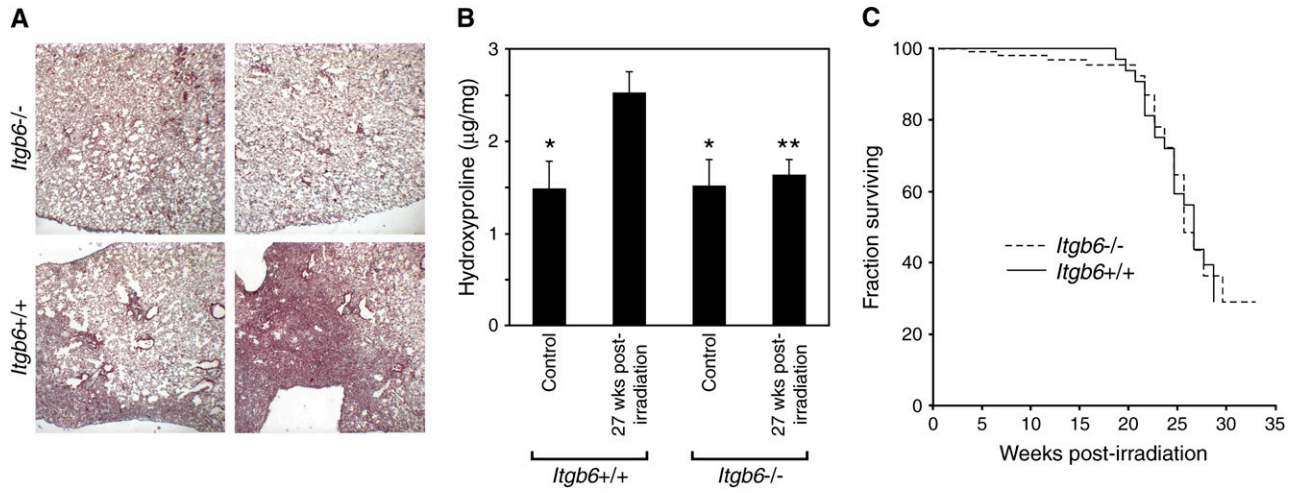

Figure 2. Mice lacking the αvβ6 integrin do not develop radiation-induced lung fibrosis. (*A*) Representative lungs from *Itgb6*$^{+/+}$ and *Itgb6*$^{-/-}$ mice (27 wk postirradiation) stained with Masson's trichrome. (*B*) Hydroxyproline content of lungs obtained from *Itgb6*$^{+/+}$ and *Itgb6*$^{-/-}$ mice (27 wk postirradiation). Hydroxyproline content of irradiated *Itgb6*$^{+/+}$ lungs is significantly greater than that of unirradiated *Itgb6*$^{+/+}$ lungs and of irradiated and unirradiated *Itgb6*$^{-/-}$ lungs (*$P < 0.03$ vs. irradiated *Itgb6*$^{+/+}$; **$P < 0.02$ vs. irradiated *Itgb6*$^{+/+}$; n = 5–6 for each group). *Error bars* represent 1 SEM. (*C*) Kaplan-Meier curves for *Itgb6*$^{+/+}$ and *Itgb6*$^{-/-}$ mice treated with a 14-Gy thoracic radiation.

irradiation and in mice killed at the study endpoint, 26 weeks after irradiation.

Mice treated with PBS, control IgG, or 0.3 mg/kg/week 6.3G9 developed fibrosis of similar extent (Figure 3A). In contrast, mice treated with 5 mg/kg/week rsTGF-βRII-Fc or 1 or 10 mg/kg/week 6.3G9 had significant reductions of histologically defined areas of fibrosis, measured as %FA. Treatment also reduced the fraction of mice with any degree of fibrosis on histologic analysis, from 17/24 and 10/14 for control IgG and PBS groups, respectively, to 14/24, 3/23, 3/21, and 10/27 for the 0.3, 1.0, and 10.0 mg/kg/week 6.3G9 and rsTGF-βRII-Fc groups, respectively ($P = 0.55$, $P < 0.0001$, $P = 0.0002$, and $P = 0.025$, respectively, compared with IgG control [Fisher's exact test]).

To assess the inflammatory response in the different treatment groups, we performed cell counts on BAL fluid obtained from mice surviving until being killed. Total cell counts were not significantly different among groups (data not shown). Differential cell counts, however, showed a nonsignificant increase in the percentage of lymphocytes at lower doses of 6.3G9 (0.3 and 1 mg/kg/wk) and with rsTGF-βRII-Fc, and a prominent increase in lymphocytes and neutrophils at 10 mg/kg/week 6.3G9 (Figure 3B). Cytospins from high-dose 6.3G9 mice contained enlarged, foamy-appearing AMs, similar in appearance to AMs isolated from lungs of *Itgb6*$^{-/-}$ mice (Figure 3D).

We compared Kaplan-Meier survival curves for all groups of mice, and found that 50% survival was reached at 23–25 weeks (Figure 3C), compared with 26 weeks in the initial experiment (Figure 2C). There was no significant difference among all the groups ($P = 0.088$ by log-rank test of all groups), but a trend toward decreased survival in the 10 mg/kg/week 6.3G9 group was apparent.

These results confirm that murine RILF is TGF-β–dependent, and that inhibition of TGF-β or αvβ6 just before and during the fibrosis phase prevents RILF. The results also suggest a potentially important difference in the effects of different 6.3G9 doses. Although both the 1 and 10 mg/kg/week doses of 6.3G9 prevent RILF, only the higher dose is associated with an increase in BAL lymphocytes and neutrophils. A similar increase in lung lymphocytes (three- to fourfold), but not neutrophils, occurs in untreated *Itgb6*$^{-/-}$ mice (16).

Dose–Response Assessment of 6.3G9 in RILF

We performed a second αvβ6 inhibition experiment to examine the effect of additional doses of 6.3G9 and to reexamine the effect of 6.3G9 on survival. We examined mice at longer times since irradiation (28–32 wk) to determine whether 6.3G9 treatment delays rather than prevents RILF. Injections were again started 16 weeks after irradiation, and 41–44 mice per group were irradiated.

We measured %FA in all mice that died after 20 weeks or were killed at endpoints of 28 or 32 weeks. Representative lesions in control mice are shown in Figure 4A. Compared with mice treated with control IgG, the groups treated with any dose of 6.3G9 had significant reductions in %FA (Figure 4B). The

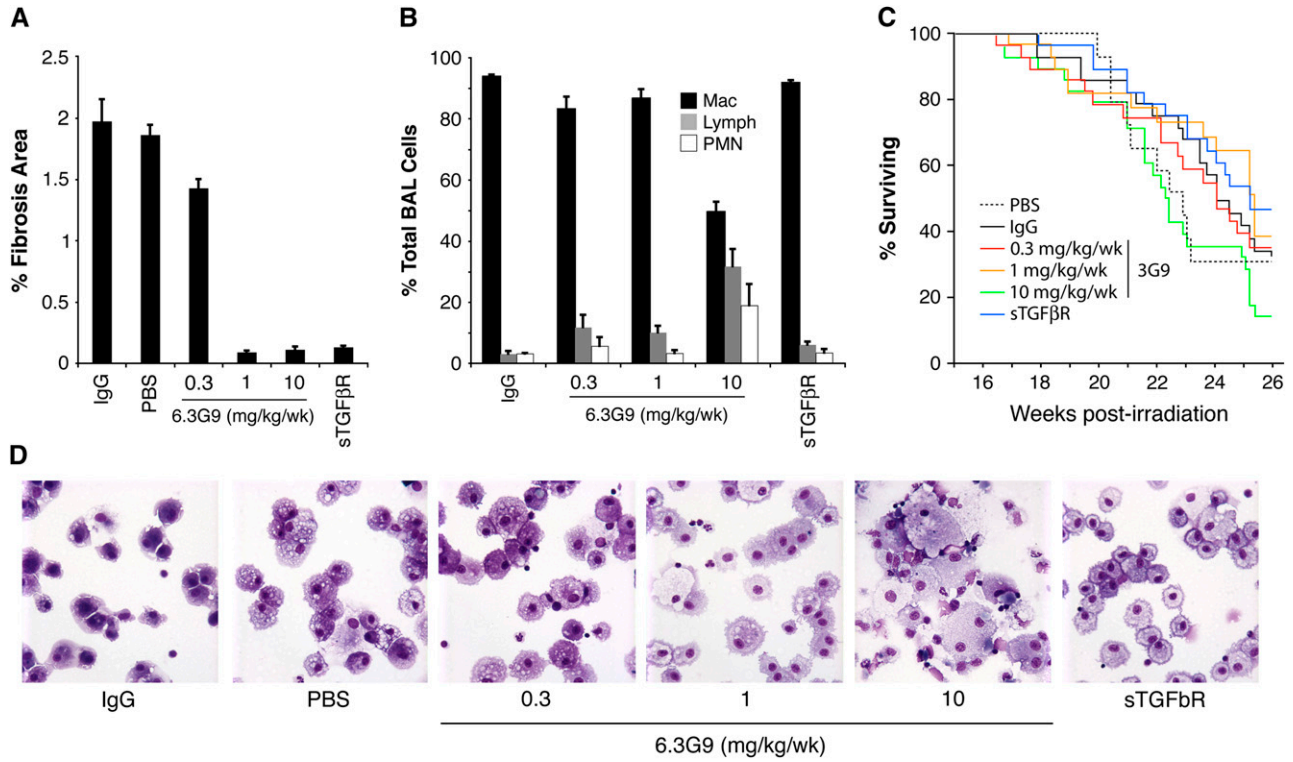

Figure 3. Effect of the anti-αvβ6 monoclonal antibody (mAb), 6.3G9, on fibrosis, lung inflammation, and survival after lung irradiation. Mice were irradiated with 14 Gy to the thorax. Weekly intraperitoneal injections with control IgG, control phosphate-buffered saline (PBS), anti-αvβ6 mAb (6.3G9), or recombinant soluble transforming growth factor-β receptor II–Fc fusion protein (rsTGF-βRII–Fc) were started 16 weeks postirradiation (n = 14–27 per group). Doses of 6.3G9 are shown; rsTGF-βRII–Fc doses were 5 mg/kg/week. (*A*) Pooled results for mice that died between 20 and 26 weeks postirradiation and mice killed at 26 weeks postirradiation. The percent fibrosis area (%FA) is significantly reduced in mice treated with 1 or 10 mg/kg/week 6.3G9 or with rsTGF-βRII–Fc, compared with IgG control ($P < 0.001$ compared with control IgG). (*B*) Differential counts of cells in bronchoalveolar lavage (BAL) fluid from mice killed 26 weeks postirradiation. (*C*) Kaplan-Meier curves for the different treatment groups during the treatment phase. Survival curves do not differ significantly in a composite analysis ($P = 0.088$ by log-rank test). (*D*) Representative cytospins of BAL cells. Enlarged macrophages and increases in other inflammatory cell types are evident in BAL fluid from mice treated with 10 mg/kg/week 6.3G9. *Error bars* represent 1 SEM.

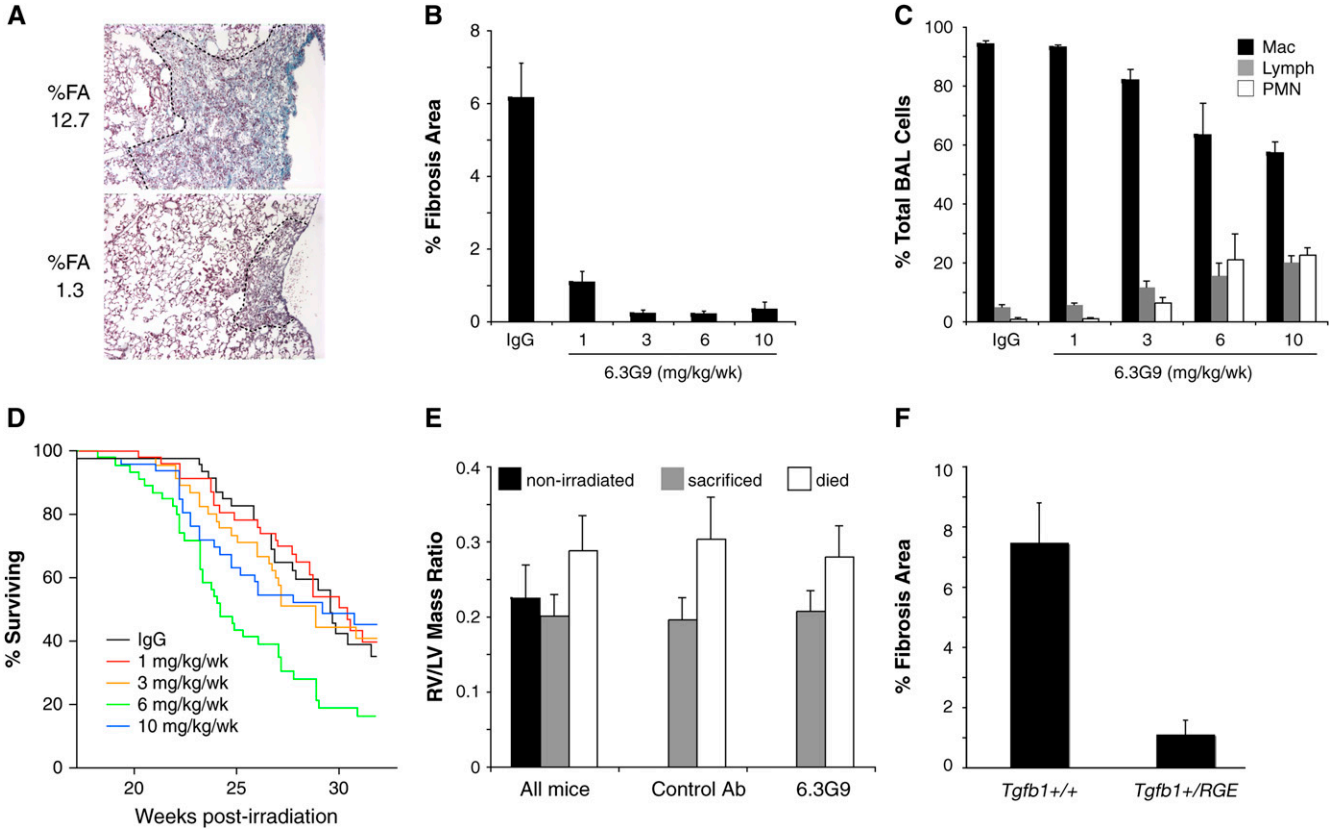

Figure 4. Analysis of additional treatment doses of anti-αvβ6 monoclonal antibody (mAb). Weekly subcutaneous injections with anti-αvβ6 mAb (6.3G9) or control IgG were started 16 weeks postirradiation (n = 14–27 per group). (*A*) Representative fibrotic lesions in two control antibody–treated, killed mice. The *dashed line* indicates the extent of the lesion. The percent fibrosis area (%FA) for the entire lung section is shown to the *left*. (*B*) Pooled results for mice that died between 20 and 32 weeks postirradiation and mice killed at either 28 or 32 weeks postirradiation. The %FA is significantly reduced by all doses of 6.3G9. (*C*) Differential counts of cells in BAL fluid obtained from mice killed at 28 or 32 weeks postirradiation. (*D*) Kaplan-Meier curves for different treatment groups during the treatment phase. Survival curves differed significantly in a composite analysis ($P < 0.005$ by log-rank test). (*E*) Comparison of right ventricle (RV):left ventricle (LV) mass ratio for mice that died between 28 and 32 weeks postirradiation versus mice that survived to be killed at 32 weeks. Results for all mice are shown on *left* with data from unirradiated controls. On *right* are data for mice treated with either control IgG or various doses of 6.3G9. For all groupings shown, mice that died had significantly increased RV:LV ratio compared with surviving mice ($P < 0.0007$) or unirradiated ($P < 0.02$) mice. (*F*) *Tgfb1*$^{+/+}$ and *Tgfb1*$^{+/RGE}$ mice were irradiated and killed 26 weeks later (n = 8 and 12, respectively). The %FA was significantly reduced in the mice heterozygous for the *Tgfb1* mutation ($P < 0.001$). *Error bars* represent 1 SEM.

%FA in mice treated with the lowest dose of 6.3G9 (1 mg/kg/wk) was 18% of control, and, in mice treated with higher doses (3–10 mg/kg/wk), was only 3–5% of control. As before, differences were also statistically significant when the numbers of samples with or without fibrosis were compared. Among control IgG-treated mice, 35/42 had histologic fibrosis; for mice treated with 1, 3, 6, or 10 mg/kg/week 6.3G9, only 25/42, 10/42, 8/42, and 9/41 mice, respectively, had histologically apparent fibrosis ($P = 0.029$ for 1 mg/kg/wk 6.3G9 and $P < 0.0001$ for the other groups, compared with the control IgG group [Fisher's exact test]).

We killed approximately equal numbers of mice 28 weeks postirradiation and collected BAL fluid for differential cell counts (19–22 mice in each group, except n = 7 for the 6 mg/kg/wk 6.3G9 group). As before, we observed a dose-dependent increase in percentages of lymphocytes and neutrophils, which were only significant at the 6 and 10 mg/kg/week doses (Figure 4C).

Survival curves for the various treatment groups are shown in Figure 4D: 50% survival was reached at 27–31 weeks postirradiation, except by the 6 mg/kg/week 6.3G9 group, for which 50% survival occurred at 24 weeks. The differences in survival curves were statistically significant ($P < 0.005$, log-rank test for all groups).

Prior studies demonstrated that RV hypertrophy (RVH) and loss of lung perfusion are late sequelae of lung irradiation (22, 23), which might explain respiratory insufficiency and death. To assess the association of RVH and lethality in our experiments, we measured the RV:LV mass ratio in three groups of mice: irradiated mice that died between 28 and 32 weeks postirradiation; mice that survived to be killed at 32 weeks; and control nonirradiated mice. The RV:LV ratio was significantly increased in mice that died, regardless of treatment status, compared with mice in the other two groups (Figure 4E).

The dose titration experiments suggested that more αvβ6-activated TGF-β is needed to cause fibrosis than to control lung inflammation. To test this hypothesis in a different way, we used mice with a knockin mutation of *Tgfb1* that eliminates TGF-β1–LAP's integrin-binding site (14). Mice homozygous for this mutation (*Tgfb1*$^{RGE/RGE}$) produce normal levels of latent TGF-β1 protein, but have a phenotype identical to that of *Tgfb*$^{-/-}$ mice. Heterozygous mice have less integrin-activatable latent TGF-β1, but have no inflammatory phenotype. We irradiated *Tgfb1*$^{+/+}$ and *Tgfb1*$^{+/RGE}$ littermates and assessed fibrosis 26 weeks after irradiation (Figure 4F). The %FA in *Tgfb1*-haploinsufficient mice was significantly less than in wild types ($P < 0.001$).

Multiplex Analysis of BAL Fluid Protein Concentrations

To further characterize the effects of anti-αvβ6 treatment in the RILF model, we measured the levels of 60 selected proteins in BAL fluid by multianalyte protein profiling. Mice from the second αvβ6 inhibition experiment, killed at 28 or 32 weeks postirradiation, were used for these measurements. The most striking finding was that many proteins in the panel, primarily inflammatory mediators, were present at significantly elevated levels in BAL fluid from irradiated mice treated with 6 and/or 10 mg/kg/week 6.3G9, compared with levels in BAL fluid from irradiated mice treated with lower doses of 6.3G9 or with control antibody. Data for four representative proteins are shown in Figures 5B and 5C. A qualitatively similar dose–response pattern was observed in nonirradiated mice treated with 6.3G9 or control mAb for 4 weeks (Figure 5A). Other proteins that were significantly elevated compared with control in the 6 and 10 mg/kg/week 6.3G9 groups, but not elevated in the 1 and 3 mg/kg/week 6.3G9 groups, were matrix metalloproteinase-9, oncostatin M, vascular endothelial growth factor, and tumor necrosis factor-α, and the chemokines granulocyte chemotactic protein (GCP)-2, IFN-inducible protein-10, and macrophage inflammatory protein-1β. Soluble CD40 and macrophage inflammatory protein-2 levels were significantly increased compared with control in mice treated with 10 mg/kg/week 6.3G9, but not in those treated with 1, 3, or 6 mg/kg/week 6.3G9. The dose–response behavior of these proteins, many of which are inflammatory mediators, closely parallels the changes in inflammatory cell counts (described previously here).

Gene Expression Analysis

We performed an Affymetrix GeneChip analysis of gene expression in lung tissue from mice treated as described in Figure 3. Lungs were collected for RNA extraction 26 weeks postirradiation. A molecular signature of an αvβ6-dependent disease mechanism was identified as a group of 595 GeneChip probesets showing significant changes in normalized signal intensity in response to both irradiation and αvβ6 blockade (*see* Table E1 in the online supplement). Hierarchical clustering (Figure 6) of the corresponding transcript expression profiles shows considerable similarity of gene expression patterns between the naive control and 1 mg/kg/week 6.3G9 groups relative to the PBS and 1E6 control groups, whereas the rsTGF-βRII-Fc and low-dose (0.3 mg/kg/wk) 6.3G9 dose had less effect on gene expression compared with the control injury (PBS and 1E6) groups. The effect of rsTGFbRII-Fc was similar to 1 mg/kg/week 6.3G9, although not as strong. These results are consistent with the decreased fibrosis observed in the 1 mg/kg/week 6.3G9 and soluble receptor treatment groups. Functional annotation of the gene list suggested a strong association of the radiation- and 6.3G9-affected genes with mechanisms involved in cell cycle regulation, especially with p21-dependent G1/S checkpoint control (data not shown). These results are similar to those obtained from microarray analysis of irradiated cells (24, 25). The cyclin-dependent kinase inhibitor, p21, an inhibitor of cell cycle progression and a mediator of apoptosis, is a target of TGF-β (26), and shows the highest fold up-regulation in lungs of irradiated mice. These results suggest that inhibition of TGF-β by either the soluble receptor or by αvβ6 blockade is effective in partially normalizing the gene expression patterns that characterize the response to radiation injury, even when treatment is initiated long after the initial insult.

DISCUSSION

TGF-β signaling is a potential therapeutic target in lung fibrosis. One approach to reducing TGF-β signaling would be to prevent activation of latent TGF-β, and we tested this strategy in the mouse RILF model. An interesting aspect of this model is the delayed and gradual onset of fibrosis, which, arguably, is more

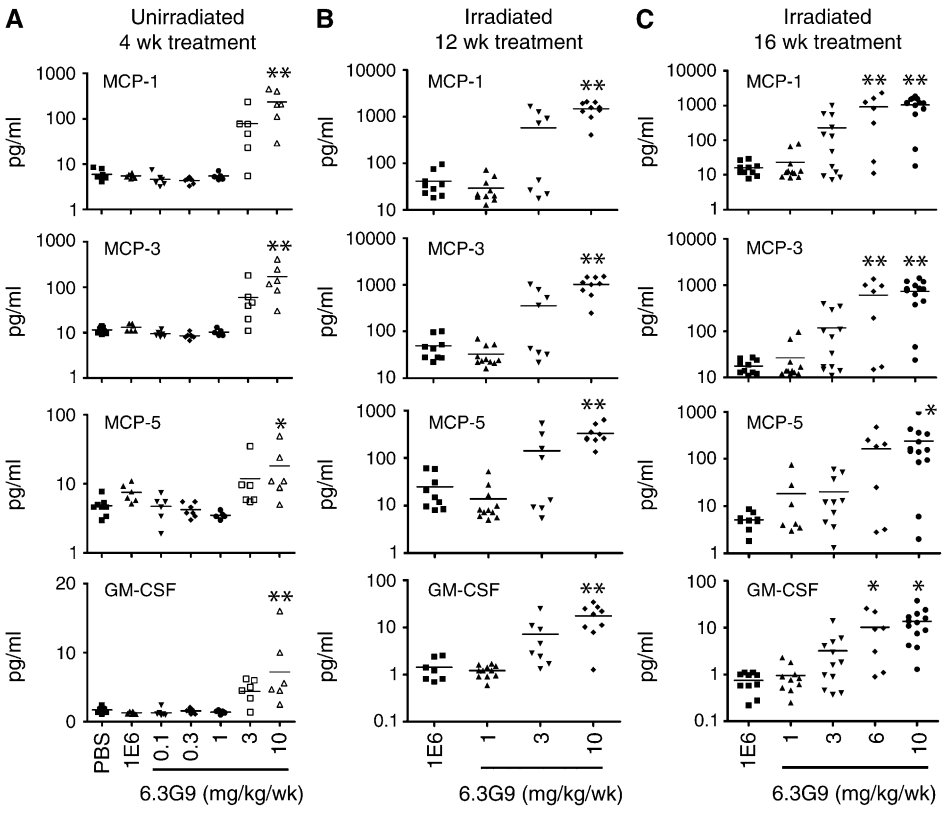

Figure 5. Differential effects of high and low doses of 6.3G9 on bronchoalveolar lavage (BAL) fluid protein concentrations. (*A*) Nonirradiated mice were treated for 4 weeks with control monoclonal antibody (mAb) or the indicated doses of 6.3G9, followed by measurement of concentrations of the indicated proteins in BAL fluid (n = 5–8 per group). (*B* and *C*) Irradiated mice were treated for 12 or 16 weeks with control mAb or indicated doses of 6.3G9, beginning 16 weeks after irradiation. The concentrations of the indicated proteins in BAL fluid obtained from these mice were then measured. $*P < 0.05$, $**P < 0.01$, compared with control antibody treatment (n = 7–13 per group).

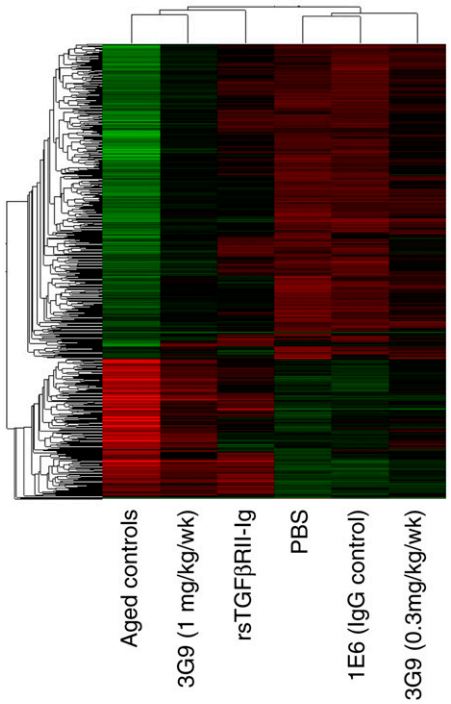

Figure 6. Microarray analysis of gene expression patterns in irradiated mice treated with 6.3G9, recombinant soluble transforming growth factor-β receptor II–Fc fusion protein (rsTGF-βRII–Fc), control IgG, or PBS. Results are from the experiment shown in Figure 3. Treatments were begun 16 weeks after irradiation, and mice were killed at 26 weeks. The selected genes shown were identified as being differentially expressed in nonirradiated mice and irradiated PBS-treated mice, and in PBS- and 1 mg/kg/week 6.3G9–treated mice. Hierarchical clustering of the gene expression data shows similarity among mice treated with PBS, control IgG, or 0.3 mg/kg/week 6.3G9 (a dose that did not prevent fibrosis). In contrast, the expression pattern of these genes in mice treated with 1 mg/kg/week 6.3G9 or rsTGF-βRII–Fc clustered with that of nonirradiated mice. Increased genes are represented by progressively brighter shades of *red,* decreased genes are represented by progressively brighter shades of *green,* and unchanged genes by *black.*

similar to human conditions, such as idiopathic pulmonary fibrosis, than is the commonly used bleomycin model. Clinically, RILF is a potential, serious complication of radiation therapy for lung carcinoma, even with careful limitation of therapeutic lung radiation doses, for which there is no known effective therapy (27).

Compared with other organs, the lung is relatively sensitive to radiation injury. Acutely, radiation causes DNA damage, with cell injury and death. Later, in a time frame of weeks to a few months after exposure, a pneumonitis phase can occur. In patients, pneumonitis is manifested by fever, cough, and infiltrates on radiographs, and often responds to corticosteroids. In rodent models, TGF-β1 expression is increased during both the acute and pneumonitis phases (28–30). At later time points (typically 5–6 mo in mice and >6 mo in humans), fibrosis can develop. Strategies to mitigate adverse radiation effects might allow treatment of lung malignancies with higher radiation doses, leading to better outcomes.

We found that αvβ6 expression is temporally, spatially, and causally linked to RILF. Up-regulation of αvβ6 in the alveolar epithelium of irradiated lung occurs just before fibrosis and persists in fibrotic lesions. In addition, *Itgb6*$^{-/-}$ mice do not develop RILF, and a specific inhibitor of αvβ6, administered just before and during the fibrosis phase of the RILF model, prevented fibrosis for up to 12 weeks after the normal time of onset. Soluble TGF-β receptor also prevented RILF. The equivalent antifibrotic efficacy of a global TGF-β inhibitor and an anti-αvβ6 inhibitor provides further evidence that αvβ6-mediated TGF-β activation is a major contributor to fibrosis. αvβ6 is now known to be involved in two distinct models of lung fibrosis (bleomycin- and radiation-induced), as well as in two models of kidney fibrosis (18, 31).

Mice lacking αvβ6 develop lymphocytic lung inflammation (16). We noted increased percentages of both lymphocytes and neutrophils in lungs of irradiated mice treated with higher doses of 6.3G9. We did not observe increased neutrophils in histologic sections of *Itgb6*$^{-/-}$ lungs after radiation exposure (data not shown). Therefore, in irradiated mice, there is an undefined inflammatory stimulus associated with high-level αvβ6 inhibition leading to accumulation of lung neutrophils that does not occur in αvβ6-null mice. The cytologic findings are mirrored by increases in several inflammation-related cytokines in BAL fluid only at doses of 6–10 mg/kg/week 6.3G9 (Figure 5). Of note, however, a 6.3G9 dose of 1 mg/kg/week prevented fibrosis without altering BAL cell counts (Figures 3 and 4) or selected inflammatory mediators (Figure 5).

There is a high mortality rate in the mouse RILF model during the fibrosis phase. Studies by Sharplin and Franko demonstrated three types of lung damage that might contribute to lethality: loss of functional acini due to obstruction by edema and hyaline membranes, extensive contracted fibrosis, and loss of lung perfusion with associated RVH (22, 23). The relative contribution of these abnormalities depends upon the mouse strain and the time since irradiation. Some strains of mice have severely reduced survival after lung irradiation in the absence of fibrosis, indicating that fibrosis is clearly not the only possible contributor to death in this model (19). However, Sharplin and Franko speculated that the extensive fibrosis in C57BL/6J mice accounts for postirradiation lethality in this mouse strain. This idea is indirectly supported by the fact that several interventions reduce both lethality and fibrosis in C57BL/6 mice exposed to lung irradiation (32–35).

In our study, the effects on fibrosis and lethality are dissociated: the dramatic prevention of fibrosis by *Itgb6* deletion or αvβ6 inhibition does not improve survival. Therefore, fibrosis does not appear to be the major cause of death in these studies. Decreased lung perfusion may be involved, because RVH was noted in mice that died during the study, but not in mice that survived, regardless of treatment. Thus, our evidence, interpreted in light of prior work (23), suggests that loss of lung perfusion occurs in C57BL/6 mice even when fibrosis is prevented, and that loss of lung perfusion is responsible at least in part for death in this model.

Radiation injury sets in motion a series of events that include vascular injury, inflammation, oxidant injury, hypoxia, and alterations in multiple signaling pathways (36, 37), which unfold over months. One consequence of these events is increased expression of αvβ6 by alveolar epithelial cells, permitting more TGF-β to be activated. Other consequences (e.g., vascular insufficiency) evidently occur upstream of, or in parallel with, αvβ6 up-regulation and fibrosis. In this view, αvβ6-mediated TGF-β activation is a more proximate cause of RILF than are factors such as oxidants, CD40/CD40L interactions, and platelet-derived growth factor signaling. Our attempts at staining for the endothelial markers, platelet endothelial cell adhesion molecule-1 and von Willebrand factor have not given us additional insight into the vascular abnormalities in these mice (data not shown). As this process is delineated, it will be interesting to determine whether the presumed vascular dysfunction in these mice is required for the αvβ6-mediated fibrotic response.

TGF-β signaling may be a component of the early events leading to increased αvβ6 expression and fibrosis, as well as a required factor in the fibrotic process. TGF-β levels in lung and serum increase in the first days after radiation injury (28, 30, 36). Short-term treatment with TGF-β antagonists at the time of irradiation reduces acute pneumonitis and, surprisingly, late-onset fibrosis at 6 months postirradiation (30, 38). Similarly, in acute lung injury, TGF-β activated by αvβ6 mediates early capillary leak (17), and is also required for subsequent fibrosis. During radiation exposure, TGF-β activation can occur by an alternate route involving direct effects of ionizing radiation on LAP (10).

Survival rates in this model are a sensitive indicator of toxicity because of the tenuous status of the mice and the long duration of treatment (up to 16 wk). We found an inconsistent tendency for high doses of 6.3G9 to worsen survival. Further studies will be needed to define whether high-dose 6.3G9 affects survival, and whether any such effect is due to enhanced inflammation or some other process.

However, our data indicate that antifibrotic efficacy is attained at doses of 6.3G9 that do not cause significant changes in BAL inflammatory cells or survival. High doses of 6.3G9 (6–10 mg/kg/wk) cause changes in BAL cell counts and macrophage morphology similar to those observed in *Itgb6*$^{-/-}$ mice, suggesting that these doses produce near-complete loss of αvβ6 function. Doses of 1–3 mg/kg/week cause minimal changes in inflammatory cell counts, while still preventing fibrosis. Importantly, although the injected doses of anti-αvβ6 mAb producing antifibrotic and proinflammatory effects differ by less than a factor of 10, the difference in circulating plasma levels achieved by these doses is significantly greater. Pharmacokinetic analyses (unpublished data) show that 6.3G9 has a significantly shorter half-life at 1 mg/kg than it does at 10 mg/kg, and the difference in exposure (measured as area under the concentration–time curve) at these two doses is approximately 80-fold. These results suggest that near-maximal antifibrotic activity is achieved at concentrations of 6.3G9 that are significantly lower than those that produce inflammatory changes in the lung.

TGF-β elicits distinct cellular responses at different concentrations (39). Our results suggest that a small amount of active TGF-β produced by αvβ6-expressing epithelium is sufficient to suppress inflammation, and a larger amount is required to cause fibrosis. These differences might be due to intrinsic differences in the responses of target cells (e.g., lymphocytes and fibroblasts), or to differences in the efficiency of active TGF-β delivery from epithelium to different target cells. In any case, the idea is supported by the observation that *Tgfb1*-haploinsufficient mice are relatively protected from RILF (Figure 4E) without any evident increase in inflammation (data not shown).

Expression of αvβ6 increases 18 weeks after radiation treatment; interestingly, plasma TGF-β levels increase sharply 18 weeks after rat lung irradiation (29). αvβ6 up-regulation also immediately precedes bleomycin-induced fibrosis (13). These correlations do not prove that high levels of αvβ6 are required for fibrosis, but adenovirus-mediated over-expression of latent TGF-β1 in normal lung does not cause fibrosis (40), suggesting that the normal lung's capacity for TGF-β activation is rate limiting for fibrosis. Increased αvβ6 expression is likely not the only way to increase αvβ6-dependent TGF-β activation; protease activated receptor-1 signals, for example, enhance αvβ6 function (41), and latent TGF-β binding protein-1 enhances activation of TGF-β by αvβ6-expressing cells (42). TGF-β increases β6 expression in cultured cells (43), but we did not find evidence for TGF-β–induced αvβ6 up-regulation in our study, because mice treated with 6.3G9 or rsTGF-βRII-Ig still had strongly up-regulated αvβ6 expression (data not shown).

Inhibition of TGF-β signaling is potentially beneficial in fibrotic and other diseases, and has been well tolerated in mice (44). Early clinical trials of TGF-β antagonists are underway. However, data from genetic mouse models indicate that reduced TGF-β activation or signaling may cause enhanced inflammation, pulmonary emphysema, and increased malignancy. Our data suggest that optimal anti–TGF-β strategies may require carefully titrated, partial inhibition of TGF-β activity to maximize benefit and minimize potential toxicity. Addressing this issue in human studies will require comparison of different dosing regimens and quantitative markers of therapeutic and adverse effects.

In summary, our data and other results indicate that the αvβ6–TGF-β axis plays a key role in various forms of lung and kidney fibrosis (13, 18). Direct inhibition of αvβ6 and, perhaps, prevention of its up-regulation are potentially useful strategies to treat or prevent RILF and other forms of fibrosis.

Conflict of Interest Statement: K.P. does not have a financial relationship with a commercial entity that has an interest in the subject of this manuscript. N.H. does not have a financial relationship with a commercial entity that has an interest in the subject of this manuscript. S.C.J. does not have a financial relationship with a commercial entity that has an interest in the subject of this manuscript. E.B. does not have a financial relationship with a commercial entity that has an interest in the subject of this manuscript. Z.Z. does not have a financial relationship with a commercial entity that has an interest in the subject of this manuscript. Z.Y. does not have a financial relationship with a commercial entity that has an interest in the subject of this manuscript. M.L.D. does not have a financial relationship with a commercial entity that has an interest in the subject of this manuscript. G.S.H. is an employee of Biogen Idec and receives annual compensation of salary and stock. P.H.W. is an employee and shareholder of Biogen Idec. M.E.L. is an employee of Biogen Idec and receives annual compensation of salary and stock. S.M.V. is an employee of Biogen Idec and receives annual compensation of salary and stock. K.S.G. does not have a financial relationship with a commercial entity that has an interest in the subject of this manuscript. C.C. does not have a financial relationship with a commercial entity that has an interest in the subject of this manuscript. S.C.F. does not have a financial relationship with a commercial entity that has an interest in the subject of this manuscript. J.S.M. received a research grant from 2004 to 2007 from Biogen Idec.

Acknowledgment: The authors thank Dean Sheppard for the *Itgb6*$^{-/-}$ mice, and gratefully acknowledge Paul Rayhorn for experimental assistance.

References

1. Chapman HA. Disorders of lung matrix remodeling. *J Clin Invest* 2004; 113:148–157.
2. Flanders KC. Smad3 as a mediator of the fibrotic response. *Int J Exp Pathol* 2004;85:47–64.
3. Branton MH, Kopp JB. TGF-β and fibrosis. *Microbes Infect* 1999; 1:1349–1365.
4. Hyytiainen M, Penttinen C, Keski-Oja J. Latent TGF-β binding proteins: extracellular matrix association and roles in TGF-β activation. *Crit Rev Clin Lab Sci* 2004;41:233–264.
5. Annes JP, Munger JS, Rifkin DB. Making sense of latent TGFβ activation. *J Cell Sci* 2003;116:217–224.
6. Kojima S, Nara K, Rifkin DB. Requirement for transglutaminase in the activation of latent transforming growth factor-β in bovine endothelial cells. *J Cell Biol* 1993;121:439–448.
7. Yu Q, Stamenkovic I. Cell surface–localized matrix metalloproteinase-9 proteolytically activates TGF-β and promotes tumor invasion and angiogenesis. *Genes Dev* 2000;14:163–176.
8. Crawford SE, Stellmach V, Murphy-Ullrich JE, Ribeiro SM, Lawler J, Hynes RO, Boivin GP, Bouck N. Thrombospondin-1 is a major activator of TGF-β1 *in vivo*. *Cell* 1998;93:1159–1170.
9. Murphy-Ullrich JE, Poczatek M. Activation of latent TGF-β by thrombospondin-1: mechanisms and physiology. *Cytokine Growth Factor Rev* 2000;11:59–69.
10. Jobling MF, Mott JD, Finnegan MT, Jurukovski V, Erickson AC, Walian PJ, Taylor SE, Ledbetter S, Lawrence CM, Rifkin DB, *et al*. Isoform-specific activation of latent transforming growth factor β (LTGF-β) by reactive oxygen species. *Radiat Res* 2006;166:839–848.
11. Mu D, Cambier S, Fjellbirkeland L, Baron JL, Munger JS, Kawakatsu H, Sheppard D, Broaddus VC, Nishimura SL. The integrin αvβ8 mediates epithelial homeostasis through MT1-MMP–dependent activation of TGF-β1. *J Cell Biol* 2002;157:493–507.

12. Annes JP, Rifkin DB, Munger JS. The integrin αvβ6 binds and activates latent TGFβ3. *FEBS Lett* 2002;511:65–68.
13. Munger JS, Huang X, Kawakatsu H, Griffiths MJ, Dalton SL, Wu J, Pittet JF, Kaminski N, Garat C, Matthay MA, *et al*. The integrin αvβ6 binds and activates latent TGF-β1: a mechanism for regulating pulmonary inflammation and fibrosis. *Cell* 1999;96:319–328.
14. Yang Z, Mu Z, Dabovic B, Jurukovski V, Yu D, Sung J, Xiong X, Munger JS. Absence of integrin-mediated TGFβ1 activation in vivo recapitulates the phenotype of TGFβ1-null mice. *J Cell Biol* 2007;176: 787–793.
15. Morris DG, Huang X, Kaminski N, Wang Y, Shapiro SD, Dolganov G, Glick A, Sheppard D. Loss of integrin αvβ6–mediated TGF-β activation causes MMP12-dependent emphysema. *Nature* 2003;422: 169–173.
16. Huang XZ, Wu JF, Cass D, Erle DJ, Corry D, Young SG, Farese RV, Sheppard D. Inactivation of the integrin β6 subunit gene reveals a role of epithelial integrins in regulating inflammation in the lung and skin. *J Cell Biol* 1996;133:921–928.
17. Pittet JF, Griffiths MJ, Geiser T, Kaminski N, Dalton SL, Huang X, Brown LA, Gotwals PJ, Koteliansky VE, Matthay MA, *et al*. TGF-β is a critical mediator of acute lung injury. *J Clin Invest* 2001;107:1537–1544.
18. Hahm K, Lukashev ME, Luo Y, Yang WJ, Dolinski BM, Weinreb PH, Simon KJ, Chun Wang L, Leone DR, Lobb RR, *et al*. αvβ6 Integrin regulates renal fibrosis and inflammation in alport mouse. *Am J Pathol* 2007;170:110–125.
19. Haston CK, Zhou X, Gumbiner-Russo L, Irani R, Dejournett R, Gu X, Weil M, Amos CI, Travis EL. Universal and radiation-specific loci influence murine susceptibility to radiation-induced pulmonary fibrosis. *Cancer Res* 2002;62:3782–3788.
20. Reddy GK, Enwemeka CS. A simplified method for the analysis of hydroxyproline in biological tissues. *Clin Biochem* 1996;29:225–229.
21. Weinreb PH, Simon KJ, Rayhorn P, Yang WJ, Leone DR, Dolinski BM, Pearse BR, Yokota Y, Kawakatsu H, Atakilit A, *et al*. Function-blocking integrin αvβ6 monoclonal antibodies: distinct ligand-mimetic and nonligand-mimetic classes. *J Biol Chem* 2004;279:17875–17887.
22. Sharplin J, Franko AJ. A quantitative histological study of strain-dependent differences in the effects of irradiation on mouse lung during the early phase. *Radiat Res* 1989;119:1–14.
23. Sharplin J, Franko AJ. A quantitative histological study of strain-dependent differences in the effects of irradiation on mouse lung during the intermediate and late phases. *Radiat Res* 1989;119:15–31.
24. Zhou T, Chou JW, Simpson DA, Zhou Y, Mullen TE, Medeiros M, Bushel PR, Paules RS, Yang X, Hurban P, *et al*. Profiles of global gene expression in ionizing-radiation–damaged human diploid fibroblasts reveal synchronization behind the G1 checkpoint in a G0-like state of quiescence. *Environ Health Perspect* 2006;114:553–559.
25. Jen KY, Cheung VG. Identification of novel p53 target genes in ionizing radiation response. *Cancer Res* 2005;65:7666–7673.
26. Datto MB, Li Y, Panus JF, Howe DJ, Xiong Y, Wang XF. Transforming growth factor β induces the cyclin-dependent kinase inhibitor p21 through a p53-independent mechanism. *Proc Natl Acad Sci USA* 1995; 92:5545–5549.
27. Kong FM, Ten Haken R, Eisbruch A, Lawrence TS. Non–small cell lung cancer therapy–related pulmonary toxicity: an update on radiation pneumonitis and fibrosis. *Semin Oncol* 2005;32:S42–S54.
28. Rubin P, Johnston CJ, Williams JP, McDonald S, Finkelstein JN. A perpetual cascade of cytokines postirradiation leads to pulmonary fibrosis. *Int J Radiat Oncol Biol Phys* 1995;33:99–109.
29. Vujaskovic Z, Down JD, van Waarde MA, van Assen AJ, Szabo BG, Konings AW. Plasma TGFβ level in rats after hemithoracic irradiation. *Radiother Oncol* 1997;44:41–43.
30. Haiping Z, Takayama K, Uchino J, Harada A, Adachi Y, Kura S, Caicun Z, Tsuzuki T, Nakanishi Y. Prevention of radiation-induced pneumonitis by recombinant adenovirus-mediated transferring of soluble TGF-β type II receptor gene. *Cancer Gene Ther* 2006;13:864–872.
31. Ma LJ, Yang H, Gaspert A, Carlesso G, Barty MM, Davidson JM, Sheppard D, Fogo AB. Transforming growth factor-β–dependent and –independent pathways of induction of tubulointerstitial fibrosis in $\beta6^{-/-}$ mice. *Am J Pathol* 2003;163:1261–1273.
32. Adawi A, Zhang Y, Baggs R, Rubin P, Williams J, Finkelstein J, Phipps RP. Blockade of CD40–CD40 ligand interactions protects against radiation-induced pulmonary inflammation and fibrosis. *Clin Immunol Immunopathol* 1998;89:222–230.
33. Rabbani ZN, Anscher MS, Folz RJ, Archer E, Huang H, Chen L, Golson ML, Samulski TS, Dewhirst MW, Vujaskovic Z. Overexpression of extracellular superoxide dismutase reduces acute radiation induced lung toxicity. *BMC Cancer* 2005;5:59.
34. Tabata C, Kadokawa Y, Tabata R, Takahashi M, Okoshi K, Sakai Y, Mishima M, Kubo H. All-trans-retinoic acid prevents radiation- or bleomycin-induced pulmonary fibrosis. *Am J Respir Crit Care Med* 2006;174:1352–1360.
35. Abdollahi A, Li M, Ping G, Plathow C, Domhan S, Kiessling F, Lee LB, McMahon G, Grone HJ, Lipson KE, *et al*. Inhibition of platelet-derived growth factor signaling attenuates pulmonary fibrosis. *J Exp Med* 2005;201:925–935.
36. Hill RP. Radiation effects on the respiratory system. *BJR Suppl* 2005; 27:75–81.
37. Vujaskovic Z, Anscher MS, Feng QF, Rabbani ZN, Amin K, Samulski TS, Dewhirst MW, Haroon ZA. Radiation-induced hypoxia may perpetuate late normal tissue injury. *Int J Radiat Oncol Biol Phys* 2001;50:851–855.
38. Anscher MS, Thrasher B, Rabbani Z, Teicher B, Vujaskovic Z. Antitransforming growth factor-β antibody 1D11 ameliorates normal tissue damage caused by high-dose radiation. *Int J Radiat Oncol Biol Phys* 2006;65:876–881.
39. Wu DT, Bitzer M, Ju W, Mundel P, Bottinger EP. TGF-β concentration specifies differential signaling profiles of growth arrest/differentiation and apoptosis in podocytes. *J Am Soc Nephrol* 2005;16:3211–3221.
40. Sime PJ, Xing Z, Graham FL, Csaky KG, Gauldie J. Adenovector-mediated gene transfer of active transforming growth factor-β1 induces prolonged severe fibrosis in rat lung. *J Clin Invest* 1997;100:768–776.
41. Jenkins RG, Su X, Su G, Scotton CJ, Camerer E, Laurent GJ, Davis GE, Chambers RC, Matthay MA, Sheppard D. Ligation of protease-activated receptor 1 enhances αvβ6 integrin-dependent TGF-β activation and promotes acute lung injury. *J Clin Invest* 2006;116:1606–1614.
42. Annes JP, Chen Y, Munger JS, Rifkin DB. Integrin αvβ6–mediated activation of latent TGF-β requires the latent TGF-β binding protein-1. *J Cell Biol* 2004;165:723–734.
43. Wang A, Yokosaki Y, Ferrando R, Balmes J, Sheppard D. Differential regulation of airway epithelial integrins by growth factors. *Am J Respir Cell Mol Biol* 1996;15:664–672.
44. Yang YA, Dukhanina O, Tang B, Mamura M, Letterio JJ, MacGregor J, Patel SC, Khozin S, Liu ZY, Green J, *et al*. Lifetime exposure to a soluble TGF-β antagonist protects mice against metastasis without adverse side effects. *J Clin Invest* 2002;109:1607–1615.